BRCA1 RING Function Is Essential for Tumor Suppression but Dispensable for Therapy Resistance

Rinske Drost,[1,2] Peter Bouwman,[1,2] Sven Rottenberg,[1,2] Ute Boon,[1,2] Eva Schut,[1,2] Sjoerd Klarenbeek,[1,2] Christiaan Klijn,[1,2] Ingrid van der Heijden,[1,2] Hanneke van der Gulden,[1,2] Ellen Wientjens,[1,2] Mark Pieterse,[1,2] Aurelie Catteau,[3] Pete Green,[3] Ellen Solomon,[3] Joanna R. Morris,[3,4,*] and Jos Jonkers[1,2,*]
[1]Division of Molecular Biology
[2]Cancer Systems Biology Centre
The Netherlands Cancer Institute, Amsterdam, 1066 CX, the Netherlands
[3]Department of Medical and Molecular Genetics, King's College London, Guy's Medical School Campus, London, SE1 9RT, UK
[4]Present address: School of Cancer Sciences, College of Medical and Dental Sciences, University of Birmingham, Edgbaston, Birmingham, B15 2TT, UK
*Correspondence: j.morris.3@bham.ac.uk (J.R.M.), j.jonkers@nki.nl (J.J.)
DOI 10.1016/j.ccr.2011.11.014

SUMMARY

Hereditary breast cancers are frequently caused by germline *BRCA1* mutations. The *BRCA1*[C61G] mutation in the BRCA1 RING domain is a common pathogenic missense variant, which reduces BRCA1/BARD1 heterodimerization and abrogates its ubiquitin ligase activity. To investigate the role of BRCA1 RING function in tumor suppression and therapy response, we introduced the *Brca1*[C61G] mutation in a conditional mouse model for BRCA1-associated breast cancer. In contrast to BRCA1-deficient mammary carcinomas, tumors carrying the *Brca1*[C61G] mutation responded poorly to platinum drugs and PARP inhibition and rapidly developed resistance while retaining the *Brca1*[C61G] mutation. These findings point to hypomorphic activity of the BRCA1-C61G protein that, although unable to prevent tumor development, affects response to therapy.

INTRODUCTION

Hereditary breast and ovarian cancer cases can often be attributed to germline mutations in the *BRCA1* gene, which confer lifetime risks of up to 90% for developing breast cancer and 40%–50% for ovarian cancer (Rahman and Stratton, 1998).

The BRCA1 protein has been implicated in maintenance of genome integrity via processes as DNA replication and repair, transcriptional regulation and chromatin remodeling (Huen et al., 2010). Especially its role in error-free repair of DNA double-strand breaks (DSBs) by homologous recombination (HR) is thought to be important for its tumor suppression activity (Moynahan et al., 1999). In the absence of BRCA1, HR is

impaired and DSBs have to be repaired by more error-prone mechanisms, like nonhomologous end joining, which may lead to the increased genomic instability that characterizes *BRCA1*-mutated tumors (Moynahan et al., 2001).

HR deficiency (HRD) may also underlie the hypersensitivity of BRCA1-deficient cells to DSB-inducing agents (Bhattacharyya et al., 2000). Although *BRCA1*-mutated ovarian cancers are often sensitive to platinum-based chemotherapy, they may eventually develop resistance via secondary mutations in the *BRCA1* gene that lead to restoration of function (Swisher et al., 2008). This finding suggests the existence of a causal link between BRCA1 status and response to DSB-inducing agents. BRCA1-deficient cells are also hypersensitive to inhibition of

---

Significance

Whereas BRCA1-related cancers respond well to therapies targeting homologous recombination deficiency (HRD), resistance is a serious clinical problem. Although reversion of *BRCA1* germline mutations has been observed in resistant tumors, it is unclear which functions of BRCA1 are required for therapy resistance. Here we show that residual activity of mutant BRCA1 proteins with a dysfunctional RING domain triggers acquired resistance to PARP inhibitors and platinum drugs. Genomic instability is viewed as a potential HRD biomarker. However, we show that although mammary tumors with different *Brca1* mutations have identical genomic profiles, they respond differently to HRD-targeting therapeutics. It may therefore be useful to stratify patients according to the underlying *BRCA1* mutation and functional biomarkers such as loss of RAD51 foci formation.

poly(ADP-ribose) polymerase (PARP) (Bryant et al., 2005; Farmer et al., 2005), an enzyme involved in DNA single-strand break (SSB) repair. In the absence of PARP activity, accumulating SSBs lead to DSBs because of replication fork stalling. Whereas these DSBs are rapidly repaired by HR in normal cells, they can only be repaired by error-prone mechanisms in BRCA1-deficient cells, resulting in gross chromosomal rearrangements and cell death. Indeed, recent clinical trials have demonstrated antitumor activity of the PARP inhibitor olaparib in BRCA1-associated cancer with only few side-effects (Fong et al., 2009, 2010; Tutt et al., 2010).

BRCA1 is a large nuclear protein that contains an N-terminal RING domain required for heterodimerization of BRCA1 with BARD1. The BRCA1/BARD1 heterodimer has E3 ubiquitin ligase activity with the class of UbcH5 E2 ubiquitin conjugating enzymes (Mallery et al., 2002; Xia et al., 2003). BRCA1/BARD1-dependent ubiquitin conjugates occur at sites of DNA DSBs suggesting that the BRCA1/BARD1 heterodimer is important for DNA repair and thereby for the tumor suppressive function of BRCA1 (Morris and Solomon, 2004). Heterodimerization of BRCA1 and BARD1 is also important for their stability in vivo (Hashizume et al., 2001; Joukov et al., 2001) and their nuclear localization (Fabbro et al., 2002).

The BRCA1/BARD1 heterodimer appears to be important for the tumor suppressor activity of BRCA1, because mammary-specific inactivation of either BRCA1 or BARD1 in mice induces mammary tumors with similar kinetics and histological features (Shakya et al., 2008). Several germline mutations within the RING finger domain of BRCA1 have been linked to development of breast and ovarian cancers (Castilla et al., 1994; Friedman et al., 1994). The C61G mutation in the BRCA1 RING domain is one of the most frequently reported missense variants (BIC database; http://research.nhgri.nih.gov/bic/) and reduces the binding between BRCA1 and BARD1. This mutation also disrupts the interaction of BRCA1 with E2 ubiquitin conjugating enzymes and thereby abrogates the E3 ubiquitin ligase activity of the BRCA1/BARD1 heterodimer (Hashizume et al., 2001; Mallery et al., 2002; Ruffner et al., 2001).

In this study we set out to investigate the importance of the RING domain for the various in vivo functions of BRCA1 and its potential importance in therapy response.

RESULTS

Embryonic Lethality of $Brca1^{C61G}$ Mutant Mice

To analyze the physiological role of the BRCA1 RING domain in mammalian cells, we generated $Brca1^{C61G}$ knock-in mice carrying a substitution of a conserved RING cysteine (Cys; TGT) into a glycine (Gly; GGT) at amino acid position 61 (Figure 1). This enabled us to exactly reproduce the human $BRCA1^{C61G}$ mutation in the mouse $Brca1$ gene.

To determine the effects of $Brca1^{C61G}$ expression on normal mouse development, we investigated whether homozygous $Brca1^{C61G}$ mice were viable. Intercrossing of heterozygous $Brca1^{C61G}$ mice did not yield $Brca1^{C61G}$ homozygous pups (Table S1 available online), indicating that the $Brca1^{C61G}$ mutation leads to embryonic lethality due to loss of BRCA1 RING function. To study at which stage of development homozygous $Brca1^{C61G}$ mice die, embryos were harvested at several time

points after gestation and genotyped. Although homozygous $Brca1^{C61G}$ embryos were still recovered at Mendelian ratios at embryonic day (E) 10.5 (Table S1), they were already severely delayed in development at E9.5 compared to $Brca1^{C61G/+}$ and $Brca1^{+/+}$ embryos (Figure 1E). From E12.5 on, $Brca1^{C61G/C61G}$ embryos could no longer be detected (Table S1). In line with this, BRCA1-deficient mouse embryonic stem (ES) cells expressing human BRCA1-C61G showed a proliferation defect, which was independent of p53 status and not caused by reduced expression levels of BRCA1-C61G protein (Figure S1).

Mammary Tumor Development in $K14cre;Brca1^{F/C61G};p53^{F/F}$ Mice

To study the role of BRCA1 RING function in tumor suppression, we introduced the $Brca1^{C61G}$ allele into the $K14cre;Brca1^{F/F};p53^{F/F}$ (KB1P) mouse mammary tumor model, in which Cre recombinase-mediated deletion of $Brca1^F$ and $p53^F$ alleles is induced in several epithelial tissues including skin and mammary gland epithelium (Liu et al., 2007). $Brca1^{C61G}$ mice were crossed with KB1P mice to generate cohorts of $K14cre;Brca1^{F/C61G};p53^{F/F}$ (KB1C61GP) mice and KB1P control littermates, which were monitored for spontaneous tumor formation. Whereas KB1P mice showed a median tumor-free survival of 236 days, KB1C61GP mice developed tumors with a significantly shorter median latency of 197 days (Figure 2A; log rank test p = 0.0003). However, when we scored for mammary tumors only, no significant difference in tumor-free survival was observed (Figure 2B; log rank test p = 0.5657). When only skin tumors were taken into account, median tumor-free survival of KB1C61GP animals was again significantly reduced compared to KB1P mice (Figure S2; log rank test p = 0.0117), showing that the difference in median tumor-free survival between KB1C61GP and KB1P mice is mainly due to skin tumors rather than mammary tumors. Although the frequency of mammary tumors was comparable for KB1C61GP and KB1P mice (63% versus 59%, respectively), the incidence of skin tumors was markedly lower in KB1C61GP mice than in KB1P mice (47% versus 75%; Figure 2C). Consequently, KB1P mice more often carried both mammary and skin tumors (37%) than KB1C61GP mice (13%).

Characterization of $K14cre;Brca1^{F/C61G};p53^{F/F}$ Mammary Tumors

On the basis of their histomorphological characteristics, the majority of mammary tumors that developed in both KB1P (89%) and KB1C61GP animals (87%) were classified as poorly differentiated solid carcinomas (Figure S3). In both groups only a small percentage of tumors were classified as carcinosarcomas, characterized by the presence of spindle-shaped cells (KB1C61GP: 2%; KB1P: 7%; Figure S3). Other tumors that developed in KB1C61GP and KB1P mice were grouped as lumen-forming carcinomas with varying degrees of glandular differentiation (Figure S3). Similar to human BRCA1-associated breast cancer (Lakhani et al., 2002), most KB1C61GP and KB1P mammary tumors stained (partly) positive for cytokeratin 8 and negative for vimentin, ER and PR (Figure 3A; Table S2).

Human BRCA1-associated breast tumors are known to display a high degree of genomic instability (Tirkkonen et al., 1997) and also mouse KB1P tumors have a considerably higher
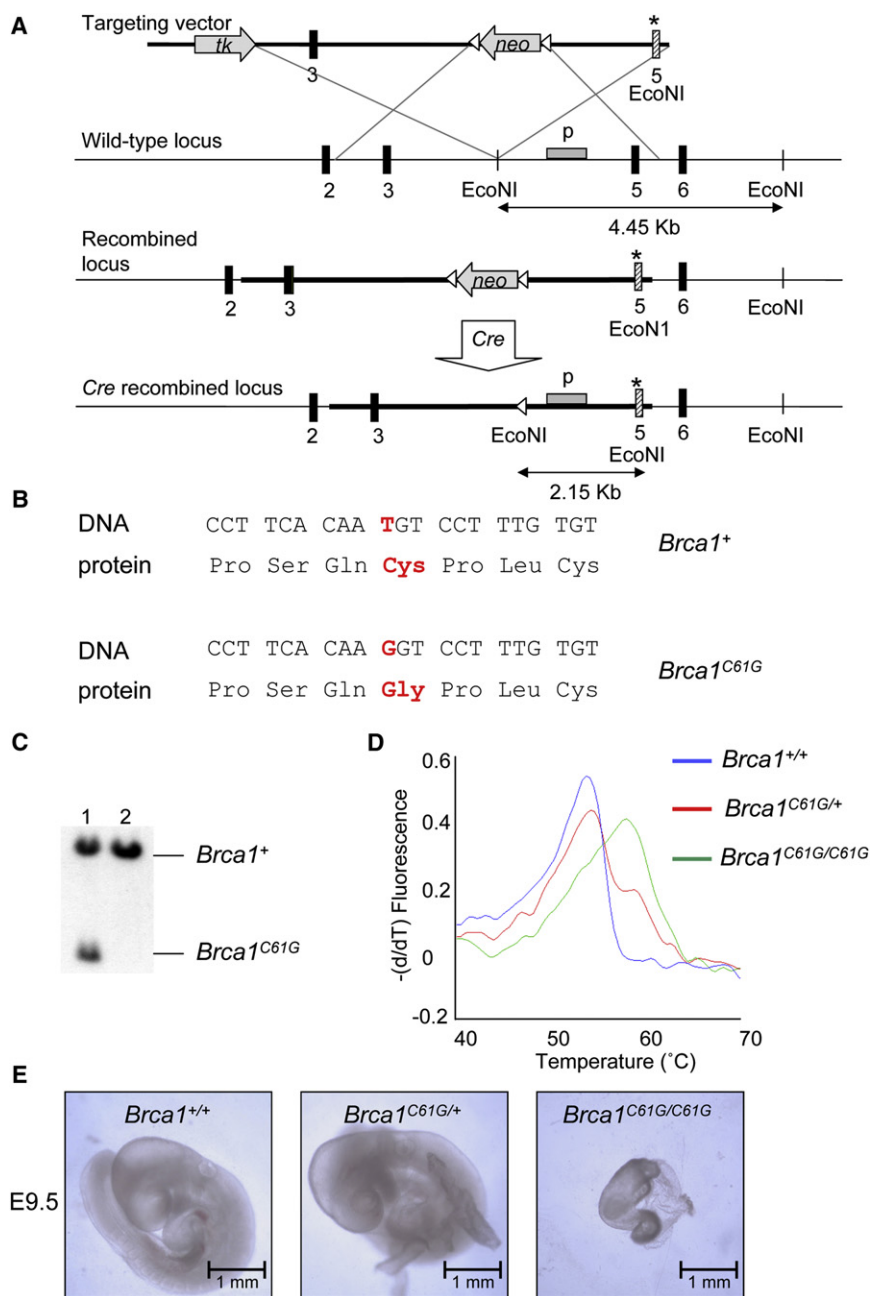
Figure 1. Embryonic Lethality of *Brca1^{C61G}* Mutant Mice

(A) Schematic overview of the *Brca1^{wt}* and *Brca1^{C61G}* allele before and after *Cre*-mediated excision of the neomycin (neo) selection marker. The *Brca1^{C61G}* mutation is indicated with an asterisk. EcoN1 restriction sites are depicted. tk, thymidine kinase negative selection cassette; *Cre*, *Cre* recombinase; p, *Brca1* intron 4 probe.

(B) Mouse *Brca1^+* and *Brca1^{C61G}* DNA and protein sequence. Location of mutation and corresponding change of amino acid residue are indicated.

(C) Southern blot analysis of *Brca1^{C61G/+}* (1) and *Brca1^{+/+}* (2) genomic DNA.

(D) Melting curve genotyping of *Brca1^{+/+}* (blue), *Brca1^{C61G/+}* (red), and *Brca1^{C61G/C61G}* (green) mice.

(E) Embryonic lethality of *Brca1^{C61G/C61G}* mice. Pictures of *Brca1^{+/+}*, *Brca1^{C61G/+}*, and *Brca1^{C61G/C61G}* mice at embryonic day 9.5 (E9.5). See also Table S1 and Figure S1.

ings, *KB1P* tumors were found to be more genomically unstable than *KP* tumors (Wilcoxon rank sum test p = 0.04632). *KB1C61GP* tumors also had a significantly higher level of genomic instability than *KP* tumors (Wilcoxon rank sum test p = 0.008207), and no significant differences could be detected between *KB1C61GP* and *KB1P* tumors (Wilcoxon rank sum test p = 0.4383). Thus, the histological features and aCGH profiles of *KB1C61GP* mammary tumors are indistinguishable from those of *KB1P* control tumors.

Whereas some studies have suggested that the *BRCA1^{C61G}* mutation leads to reduced BRCA1 stability due to disruption of the BRCA1-BARD1 interaction (Hashizume et al., 2001; Joukov et al., 2001), others have found that the mutation has only a slight impact on BRCA1 stability (Brzovic et al., 2001; Nelson and Holt, 2010). To test the effect of the *Brca1^{C61G}* mutation on protein stability, several *KB1C61GP* and control tumors were analyzed for BRCA1 protein expression by western blot (Figure 3D). *KB1C61GP* and control *KP* tumors expressed BRCA1 protein at similar levels, indicating no significant instability of the murine BRCA1-C61G protein.

Response of *K14cre;Brca1^{F/C61G};p53^{F/F}* Mammary Tumors to the PARP Inhibitor Olaparib

Mammary tumors arising in the *KB1P* mouse model can be transplanted orthotopically into female wild-type mice without losing their histomorphological features, molecular characteristics, and drug sensitivity profile (Rottenberg et al., 2007, 2010). We used this transplantation system to study the response of *KB1C61GP* mammary tumors to the clinical PARP inhibitor
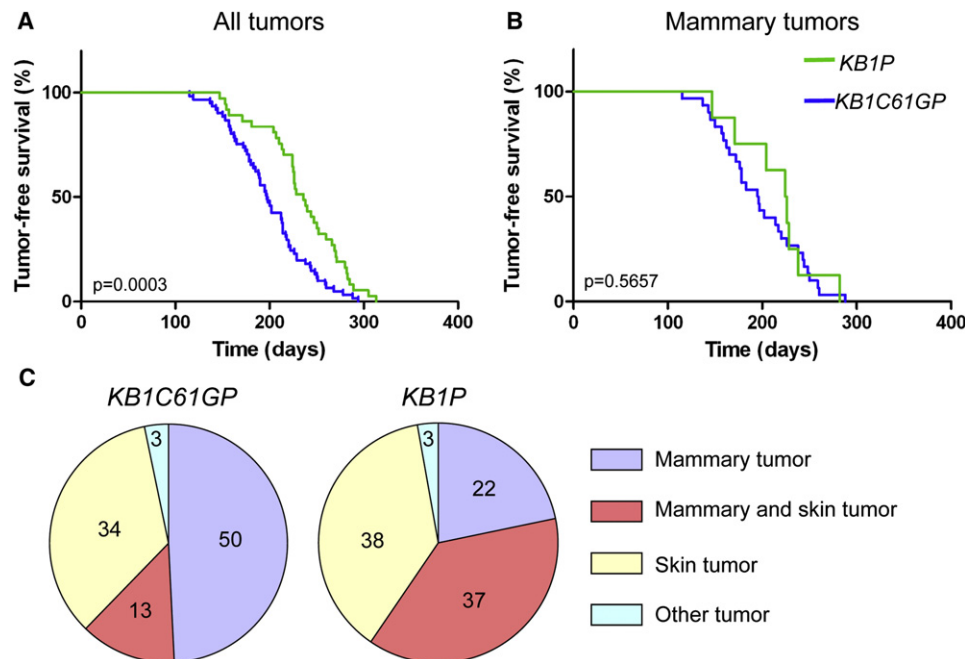
number of genomic alterations than tumors from *K14cre;p53^{F/F}* (*KP*) mice (Holstege et al., 2010; Liu et al., 2007). To investigate the level of genomic instability in *KB1C61GP* tumors, we measured DNA copy number aberrations (CNAs) in mammary tumors from *KB1C61GP* (n = 20), littermate *KB1P* (n = 18) and *KP* mice (n = 19) using array comparative genomic hybridization (aCGH). When applying the comparative module of the R package KCsmart (de Ronde et al., 2010; Klijn et al., 2008), we did not find any differences between recurrent CNAs of *KB1C61GP* and *KB1P* tumors (Figure 3B). We also counted the number of segments per individual tumor as a measure of genomic instability and aggregated the results of individual tumors per genotype (Figure 3C). In line with our previous find-

Figure 2. Spontaneous Tumor Development in *KB1C61GP* and *KB1P* Mice

(A) Tumor-free survival of *KB1C61GP* mice (*K14cre;Brca1$^{F/C61G}$;p53$^{F/F}$*; blue curve; T$_{50}$ = 197 days, n = 61 mice) and *KB1P* mice (*K14cre;Brca1$^{F/F}$;p53$^{F/F}$*; green curve; T$_{50}$ = 236 days, n = 37 mice). T$_{50}$: median tumor-free survival; n, number of mice.

(B) Mammary tumor-free survival *KB1C61GP* (blue; T$_{50}$ = 196 days, n = 30 mice) and *KB1P* mice (green; T$_{50}$ = 225 days, n = 8 mice).

(C) Distribution of different tumor types in *KB1C61GP* and *KB1P* mice. Purple, only one or multiple mammary tumor(s); yellow, only one or multiple skin tumor(s); orange, both mammary and skin tumor(s); blue, another kind of tumor. See also Figure S2.

olaparib (AZD2281). Several independent *KB1C61GP*, *KB1P*, or *KP* tumors were transplanted into the fourth mammary gland of syngeneic recipient females and tumor-bearing mice were either treated with olaparib or left untreated (Figure 4A). In all cases, untreated animals had to be sacrificed within 12 days because of a large tumor (Figure 4B, left panel; Figure S4). No significant differences in overall survival (OS) after transplantation could be observed between *KP*, *KB1C61GP*, and *KB1P* tumors (*KP* versus *KB1C61GP*: log rank test p = 0.1953; *KB1C61GP* versus *KB1P*: log rank test p = 0.1210). Whereas mice carrying *KP* tumors did not respond to olaparib treatment (Figures 4B and 4C, red curves; Figure S4), the median survival of mice carrying *KB1P* tumors increased from 12 to 60 days following treatment with olaparib and their tumors disappeared during treatment (Figures 4B and 4C, green curves; Figure S4). However, as reported before (Rottenberg et al., 2008), *KB1P* tumors could not be eradicated with this 28-day dosing schedule and all tumors grew back after the end of treatment. Interestingly, mice transplanted with *KB1C61GP* tumors had an average OS of 23 days after start of treatment (Figure 4B, right panel, blue curve), which was significantly better than *KP* tumors, but significantly worse than *KB1P* tumors (*KP* versus *KB1C61GP*: log rank test p = 0.0002, *KB1C61GP* versus *KB1P*: log rank test p = 0.006). In contrast to *KB1P* tumors, *KB1C61GP* tumors never shrank in response to olaparib treatment, but continued to grow after a short period of tumor stasis (Figure 4C). These data indicate that, whereas *KB1C61GP* and *KB1P* tumors have similar characteristics, their responses to olaparib differ substantially.

Response of *K14cre;Brca1$^{F/C61G}$;p53$^{F/F}$* Mammary Tumors to Cisplatin

We also investigated the response of *KB1C61GP* tumors to the maximum tolerable dose (MTD) of cisplatin, to which *KB1P* tumors never develop complete resistance (Rottenberg et al., 2007). We again transplanted several individual *KB1C61GP*, *KB1P*, and *KP* mammary tumors and treated tumor-bearing mice with cisplatin (Table S3; Figure 5A). Because cisplatin can have toxic side effects after multiple rounds of treatment, we studied both OS and tumor-free survival (TFS). Although the median OS of mice transplanted with *KP* tumors was prolonged from 11 to 48 days following cisplatin treatment (Figure 5B, red curve), they quickly developed resistance (Figure S5A). Consequently, 38% of the mice transplanted with *KP* tumors had to be sacrificed because of resistance (Figure 5C). As described before (Rottenberg et al., 2007), *KB1P* tumors respond well to platinum therapy, showing an increase in median OS from 12 days to 196 days following cisplatin treatment (Figure 5B, green curve). *KB1P* tumors never developed resistance and ultimately all animals had to be sacrificed because of toxicity (Figure 5C; Figure S5A). Remarkably, mice transplanted with *KB1C61GP* tumors showed a significantly worse OS after cisplatin therapy than mice transplanted with *KB1P* tumors (Figure 5B; Figure S5B; *KB1C61GP*: T$_{50}$ = 70 days; *KB1P*: T$_{50}$ = 196 days; log rank test p = < 0.0001). This difference in survival was even more pronounced when only animals that had to be sacrificed because of a large tumor were scored (Figure S5C; log rank test p = < 0.0001). Moreover, *KB1C61GP* tumors readily
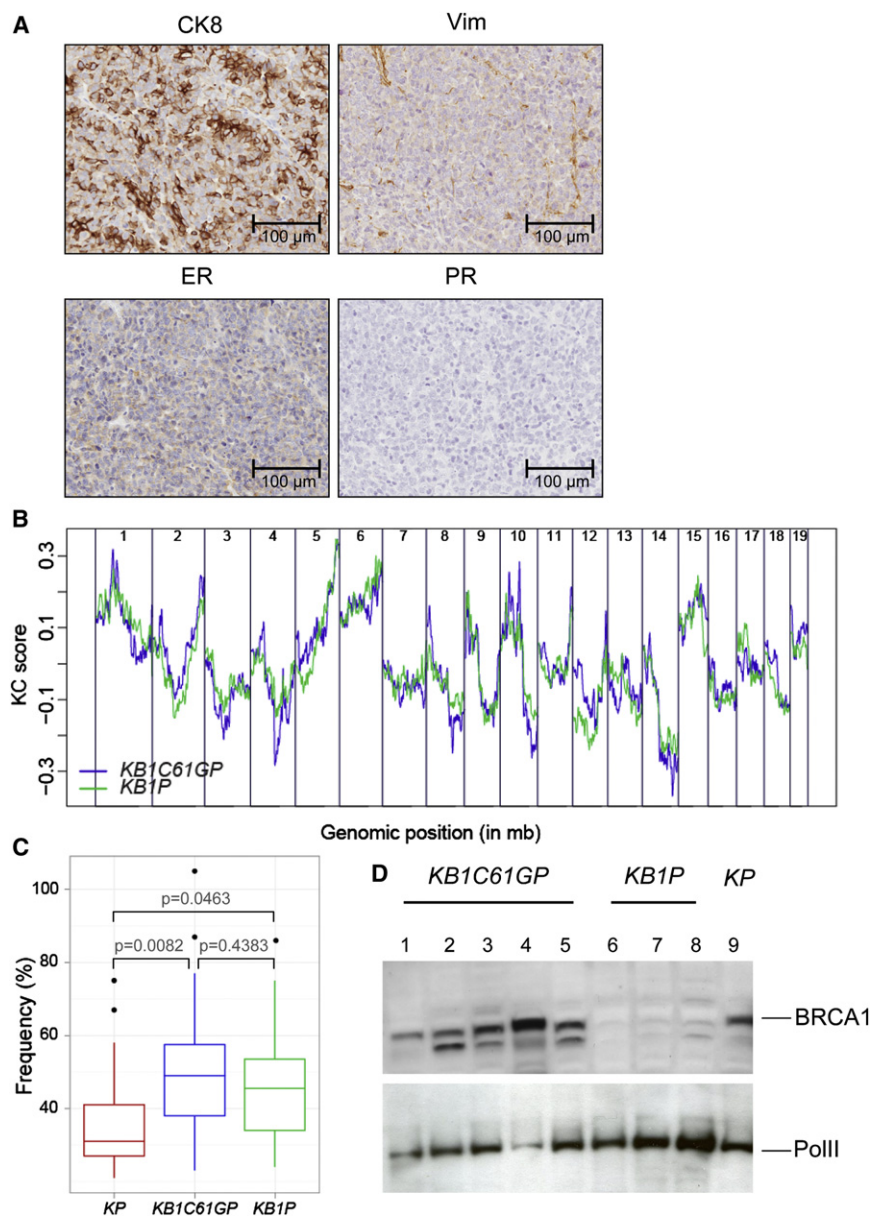
Figure 3. Molecular Characterization of *KB1C61GP* Mouse Mammary Carcinomas

(A) Immunohistochemical staining of sections from a *KB1C61GP* solid mouse mammary carcinoma for cytokeratin 8 (CK8), vimentin (Vim), estrogen receptor (ER), and progesterone receptor (PR).

(B) Comparative KC-Smart profiles of 20 *KB1C61GP* (blue) and 18 *KB1P* (green) mouse mammary carcinomas. Chromosome numbers are represented on the x axis, KC score (measure of recurrence and strength of copy number change over a group of tumors) is depicted on the y axis.

(C) Level of genomic instability in *KB1C61GP* mouse mammary carcinomas. The graph displays the number of discrete copy number aberrations identified by segmentation of aCGH profiles from BRCA1-proficient *K14cre;p53$^{F/F}$* (*KP*) tumors (red boxplot), *KB1C61GP* tumors (blue boxplot), and *KB1P* tumors (green boxplot). The size of the box represents the variation between tumors within a group and the line within the box depicts the average level of genomic instability. Errors bars indicate standard deviation (SD).

(D) BRCA1 protein expression in *KB1C61GP* mouse mammary carcinomas. Lanes 1–5, *KB1C61GP* tumors; lanes 6–8, *KB1P* littermate control tumors; lane 9, *KP* tumor. PolII protein expression was used as loading control. See also Figure S3 and Table S2.

in tumor outgrowth after retransplantation between cisplatin-sensitive and cisplatin-resistant tumors (Figure 5D, left upper panel; log rank test p = 0.2102). When tumors reached a volume of 200 mm^3, mice were treated with the MTD of cisplatin. Mice transplanted with platinum-resistant tumors responded significantly worse to cisplatin treatment than animals transplanted with platinum-sensitive tumors (Figure 5D, right upper panel; log rank test p = 0.0003), indicating that cisplatin resistance of *KB1C61GP* tumors is a stably acquired trait.

To probe whether platinum resistance in *KB1C61GP* tumors could be due to a platinum-specific mechanism such as increased nucleotide excision repair (NER) or to restoration of HR, we investigated cross-resistance of cisplatin-resistant *KB1C61GP* tumors to olaparib. Mice engrafted with cisplatin-sensitive and cisplatin-resistant *KB1C61GP* tumors were treated with 50 mg/kg olaparib for 28 successive days. Mice carrying platinum-sensitive *KB1C61GP* tumors showed a good response to olaparib, which was comparable to the response to cisplatin (Figure 5D, right upper panel and left lower panel; cisplatin T$_{50}$ = 29 days versus olaparib T$_{50}$ = 32 days). Compared to mice transplanted with platinum-sensitive tumors, mice with platinum-resistant tumors responded significantly worse to olaparib treatment, showing a median OS of only 10 days (Figure 5D, left lower panel; log rank test p = 0.0002). Thus,
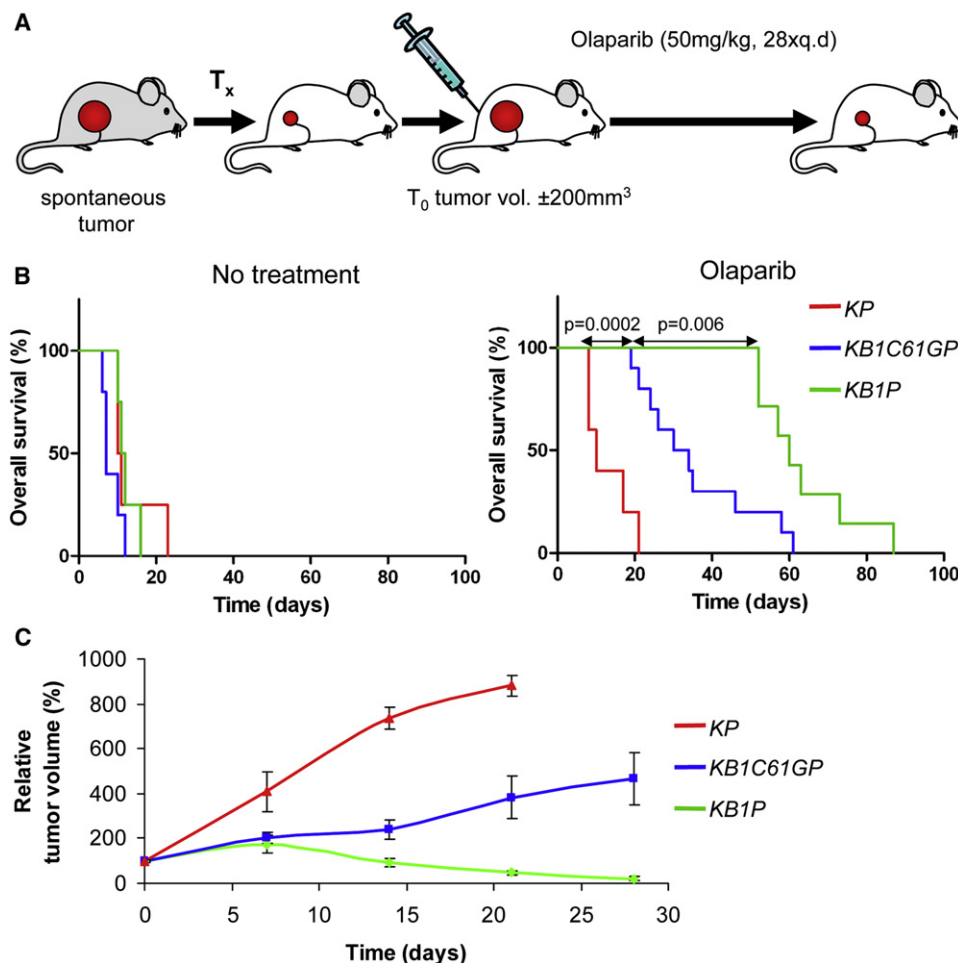
developed cisplatin resistance and 50% of the mice had to be sacrificed because of therapy-refractory tumors (Figure 5C; Figure S5D; Table S3). In fact, no significant difference in OS after cisplatin therapy was observed between mice transplanted with *KB1C61GP* and *KP* tumors, respectively (Figure 5B; log rank test p = 0.5823). Thus, the response of *KB1C61GP* tumors to cisplatin treatment is more similar to *KP* tumors than to *KB1P* tumors.

Acquired Cisplatin Resistance in *K14cre; Brca1$^{F/C61G}$;p53$^{F/F}$* Mammary Tumors

To investigate whether resistance of *KB1C61GP* tumors to cisplatin was stable, we retransplanted both platinum-sensitive and platinum-resistant tumors derived from four different *KB1C61GP* donor tumors. There was no significant difference

Figure 4. Olaparib Response of *KB1C61GP* Mammary Tumors

(A) Schematic representation of olaparib treatment schedule. T_x, orthotopic transplantation of fragments from spontaneous mouse mammary tumors; T_0, start of treatment at a tumor volume of 200 mm^3 (100%). Mice received a daily dose of 50 mg/kg olaparib intraperitoneally for 28 consecutive days.

(B) Overall survival (OS) curves of mice transplanted with *KB1C61GP* (blue), *KB1P* (green), and *KP* (red) tumors. The left graph depicts untreated animals; the right graph shows mice treated with olaparib. T_{50}, median OS; n, number of mice. *KP* without treatment: $T_{50} = 11$ days, n = 4 mice, *KP* with olaparib treatment: $T_{50} = 10$ days, n = 5 mice; *KB1C61GP* without treatment: $T_{50} = 7$ days, n = 5 mice, *KB1C61GP* with olaparib treatment: $T_{50} = 23$ days, n = 10 mice; *KB1P* without treatment: $T_{50} = 12$ days, n = 4 mice, *KB1P* with olaparib treatment: $T_{50} = 60$ days, n = 7 mice.

(C) Comparison of relative mammary tumor volumes during 28-day treatment with olaparib. Tumor volumes are relative to the tumor volume at start of treatment (day 0, 100% = ±200 mm^3). Error bars indicate standard error of the mean (SEM). See also Figure S4.

platinum-resistant *KB1C61GP* tumors display cross-resistance to olaparib.

We next investigated cross-resistance of cisplatin-resistant *KB1C61GP* tumors to the bifunctional alkylator nimustine. Bifunctional alkylators may be more lethal to HR-deficient cells than platinum agents because they are more efficient in inducing DNA interstrand crosslinks (ICLs), which can only be resolved by HR-mediated DNA repair (Deans and West, 2011). Treatment of mice carrying cisplatin-sensitive *KB1C61GP* tumors with a single dose of 48 mg/kg nimustine resulted in a median OS of 28 days, which is comparable to the median OS after treatment with cisplatin ($T_{50} = 29$ days) or olaparib ($T_{50} = 32$ days; Figure 5D). Interestingly, a similar median OS was observed following nimustine treatment of mice carrying cisplatin-resistant *KB1C61GP* tumors ($T_{50} = 24$ days) and there was no significant

difference in OS benefit from nimustine treatment between animals carrying platinum-resistant or platinum-sensitive tumors (Figure 5D, right lower panel; log rank test p = 0.7458). Thus, although cisplatin-resistant *KB1C61GP* tumors show cross-resistance to PARP inhibition, no cross-resistance to bifunctional alkylators such as nimustine was observed.

No Genetic Reversion of the *Brca1^{C61G}* Mutation in Therapy-Resistant Tumors

The cross-resistance of cisplatin-resistant *KB1C61GP* tumors to olaparib suggests that the mechanism of platinum resistance involves adaptation of HR-mediated DNA repair. Because secondary mutations in *BRCA1/2* can lead to resistance to platinum agents and olaparib in BRCA1/2-deficient cell lines and ovarian tumors (Sakai et al., 2008, 2009; Swisher et al., 2008),
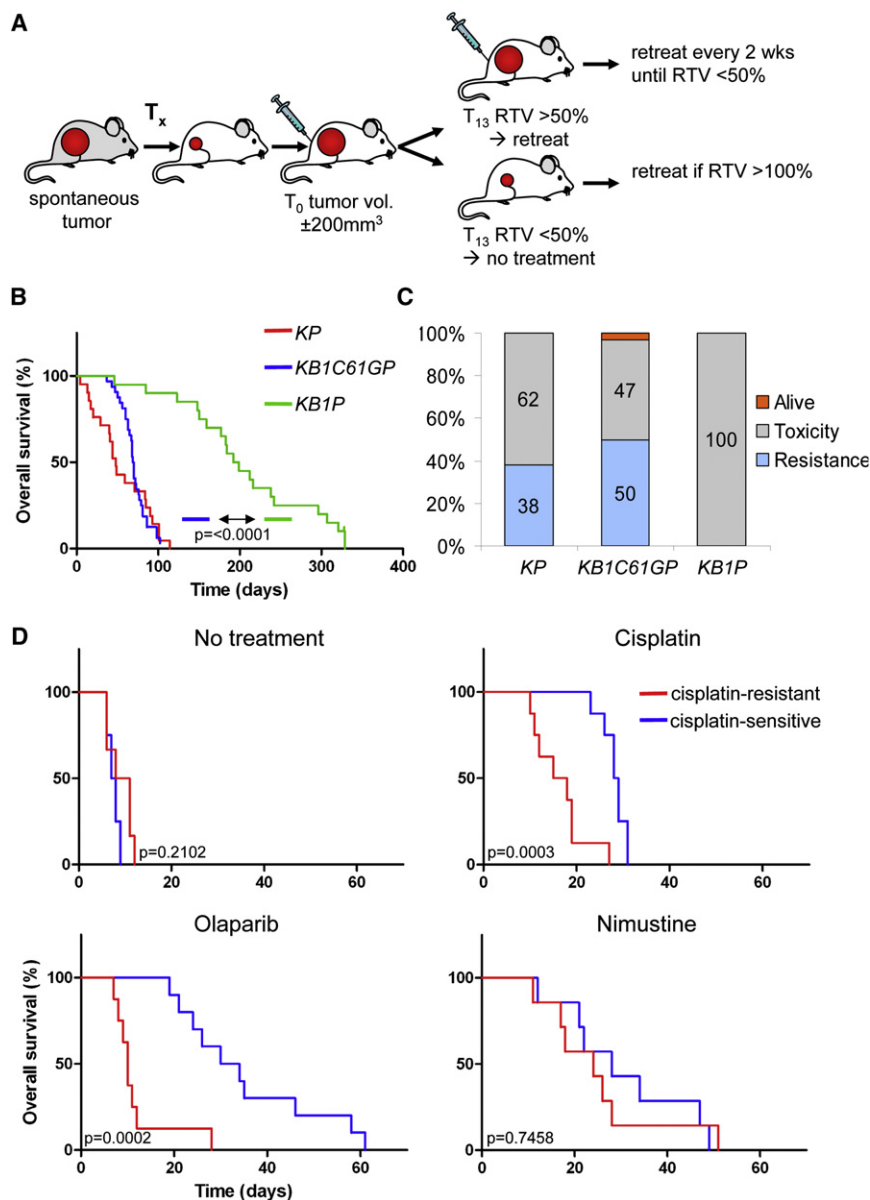
Figure 5. Cisplatin Response of *KB1C61GP* Mammary Tumors

(A) Schematic representation of cisplatin treatment schedule. T_x, orthotopic transplantation of fragments from spontaneous mouse mammary tumors. T_0, start of treatment at a tumor volume of ~200 mm³, corresponding to a relative tumor volume (RTV) of 100%. T_{13}, if the RTV on day 13 was ≥50%, mice received an additional treatment that was repeated every 2 weeks until their tumor shrank to a RTV of ≤50%. If the RTV at T_{13} was ≤50%, retreatment was postponed until the tumors grew back to their starting volume.

(B) OS curves of mice transplanted with *KB1C61GP* (blue), *KB1P* (green), and *KP* (red) tumors after cisplatin treatment. *KP*, T_{50} = 48 days, n = 21 mice; *KB1C61GP*, T_{50} = 70 days, n = 32 mice; *KB1P*, T_{50} = 196 days, n = 20 mice.

(C) Causes of death of tumor-bearing mice after treatment with cisplatin. The stacked bars depict the percentage of mice that are still alive (orange) or sacrificed because of cisplatin-associated toxicity (gray) or cisplatin-resistant tumors (blue).

(D) Effects of cisplatin, olaparib, or nimustine on OS of mice transplanted with cisplatin-sensitive (blue) and cisplatin-resistant (red) *KB1C61GP* tumors. Top left panel: OS of untreated mice (cisplatin-sensitive: T_{50} = 8 days, n = 4 mice; cisplatin-resistant: T_{50} = 10 days, n = 6 mice). Top right panel: OS after treatment with a single dose of 6mg/kg cisplatin (cisplatin-sensitive: T_{50} = 29 days, n = 8 mice; cisplatin-resistant: T_{50} = 17 days, n = 8 mice). Bottom left panel: OS after daily treatment with 50 mg/kg olaparib for 28 consecutive days (cisplatin-sensitive: T_{50} = 32 days, n = 10 mice; cisplatin-resistant: T_{50} = 10 days, n = 8 mice). Bottom right panel: OS after treatment with a single dose of 48 mg/kg nimustine (cisplatin-sensitive: T_{50} = 28 days, n = 7 mice; cisplatin-resistant: T_{50} = 24 days, n = 7 mice). See also Table S3 and Figure S5.

we investigated whether acquired resistance of *KB1C61GP* tumors was due to genetic reversion of the *Brca1^C61G* mutation. Sanger sequencing and southern blot analysis showed that all cisplatin-resistant *KB1C61GP* tumors retained the *Brca1^C61G* mutation (Figures 6A and 6B; Table S3, and data not shown). The wild-type band on the southern blot in Figure 6B is probably derived from wild-type stromal cells from the recipient animal, since PCR genotyping confirmed complete absence of the *Brca1^F* allele (data not shown). To exclude other secondary mutations in *Brca1*, we sequenced the first eight exons of mouse *Brca1* in all cisplatin-resistant tumors. Besides the *Brca1^C61G* mutation, no other mutations could be detected in the cisplatin-resistant tumors (data not shown). In conclusion, we have found no evidence for genetic reversion of the *Brca1^C61G* mutation as a mechanism of platinum resistance in *KB1C61GP* mouse mammary tumors.

Next, we evaluated potential changes in *Brca1^C61G* mRNA and protein levels in cisplatin-resistant *KB1C61GP* tumors. To avoid unwanted detection of *Brca1^Δ5-13* mRNA expression, we used primers located in the deleted part of the *Brca1* gene. The level of *Brca1^C61G* mRNA expression in untreated *KB1C61GP* tumors was comparable to the level of *Brca1* expression in BRCA1-proficient *KP* tumors (Figure 6C; Figure S6A). This corresponds to normal levels of BRCA1 protein in spontaneous *KB1C61GP* tumors (Figure 3D) and in BRCA1-deficient mouse ES cells reconstituted with human BRCA1-C61G (Figure S1B). On average, cisplatin-resistant *KB1C61GP* tumors did not show a significantly higher level of *Brca1^C61G* mRNA expression than untreated *KB1C61GP* tumors (Figure 6C; Figure S6B). However, we observed substantial heterogeneity between individual tumors, and some cisplatin-resistant tumors showed higher BRCA1 mRNA and protein expression than their untreated counterparts (Figures 6C and 6D; Figures S6A and S6B). We did not find evidence for a direct correlation between high BRCA1 expression levels
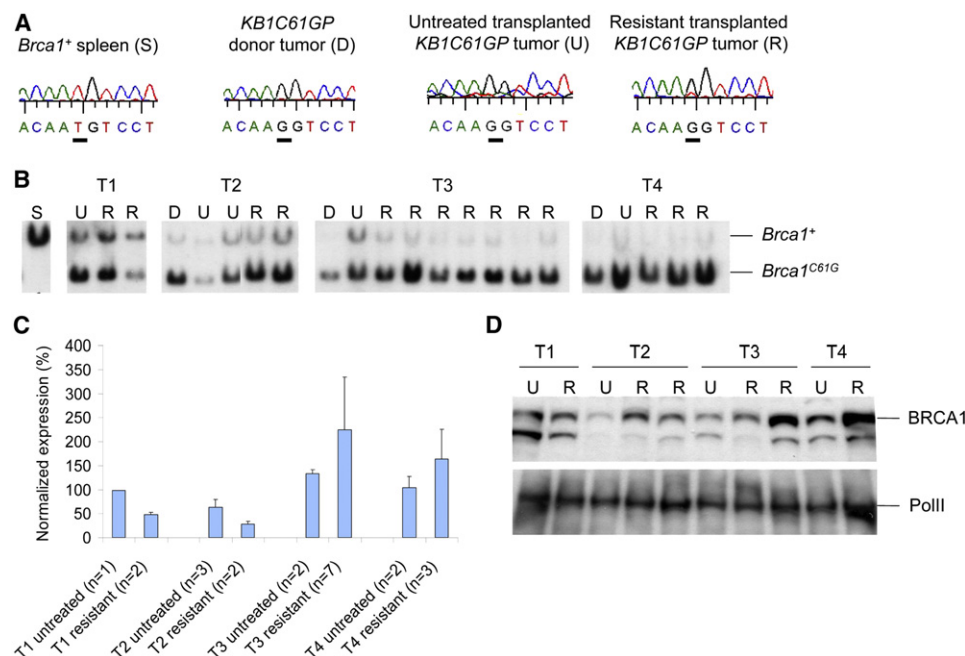
Figure 6. No Genetic Reversion in Cisplatin-Resistant *KB1C61GP* Mammary Tumors
(A) Sanger sequencing of DNA from *KB1C61GP* tumors shows that the c.181T > G mutation in the *Brca1^C61G* allele is retained in cisplatin-resistant tumors.
(B) Southern blot analysis of DNA from normal spleen (S) and *KB1C61GP* tumors. D, spontaneous donor tumors; U, untreated transplanted tumors; R, cisplatin-resistant transplanted tumors. T1, T2, T3, and T4 represent individual spontaneous *KB1C61GP* donor tumors. Transplanted tumors were grouped according to the *KB1C61GP* donor tumor from which they originated.
(C) *Brca1* qRT-PCR of untreated and cisplatin-resistant transplanted *KB1C61GP* tumors. *Brca1* mRNA expression was normalized to mRNA expression of a housekeeping gene (HPRT). *Brca1* mRNA expression in a *KP* mammary tumor was set at 100%. Error bars indicate SD. n, number of tumors.
(D) Western blot analysis of untreated (U) and cisplatin-resistant (R) *KB1C61GP* tumors. PolII protein expression was used as loading control. See also Figure S6.

and poor therapy response. Thus, the relevance of increased BRCA1-C61G expression for the development of platinum resistance remains unclear.

It was recently shown that BRCA1-deficient breast cancers show derepression of satellite DNA transcription, which may contribute to tumorigenesis through induction of genomic instability (Zhu et al., 2011). Presumably, repression of satellite DNA transcription may also serve as a mechanism of therapy resistance in BRCA1-deficient cancers. We could, however, not observe significant differences in satellite repeat expression between BRCA1-proficient *KP* tumors, BRCA1-deficient *KB1P* tumors and *KB1C61GP* tumors (Figure S6C). In addition, satellite repeat expression between cisplatin-sensitive and cisplatin-resistant tumors was not significantly different (Figure S6C).

Hypomorphic Activity of BRCA1-C61G
The poor initial response to olaparib and normal BRCA1 protein expression in *KB1C61GP* tumors prompted us to compare their intrinsic DNA repair capacity to BRCA1-proficient *KP* tumors and BRCA1-deficient *KB1P* tumors. Several *KB1C61GP, KP*, and *KB1P* tumors were transplanted and treated with cisplatin or olaparib when they reached a volume of ~200 mm³ (Rottenberg et al., 2008). Mice were sacrificed 24 hr after they received a single dose of cisplatin or 2 hr after receiving the last of seven daily doses of olaparib. Subsequently, the level of apoptosis, proliferation, and DSBs were evaluated by immunohistochemistry for cleaved caspase 3, ki67, and pH2AX, respectively. No

difference in the level of apoptosis and proliferation could be observed between *KB1C61GP*, *KP*, and *KB1P* tumors, regardless of treatment (data not shown). Also the level of DSBs did not differ significantly between untreated *KB1C61GP*, *KP*, and *KB1P* tumors (Figures 7A and 7B). As expected, the number of DSBs increased considerably after treatment with cisplatin for all tumor groups (Figures 7A and 7B). In line with the hypersensitivity of BRCA1-deficient *KB1P* tumors to olaparib (Rottenberg et al., 2008), the number of pH2AX-positive cells was significantly higher in olaparib-treated *KB1P* tumors than in *KP* tumors (Figures 7A and 7B, unpaired t test p = 0.0002). Remarkably, the level of DSBs after olaparib treatment was significantly lower in *KBC61GP* tumors than in *KB1P* tumors (unpaired t test p = 0.0020), suggesting that the DNA damage response is (partially) intact in *KB1C61GP* tumor cells. However, BRCA1-C61G expression alone may not be sufficient to mediate this response, since BRCA1-deficient ES cells expressing BRCA1-C61G do not show functional HR activity and are still sensitive to cisplatin and olaparib (Figures S7A–S7D).

To evaluate whether the decreased amount of damage-induced DSBs in *KB1C61GP* tumors could be due to an altered DNA damage response in vivo, we assessed the formation of irradiation-induced RAD51 foci (RAD51 IRIFs) in short-term tumor cell cultures derived from the different tumor genotypes. As expected, RAD51 IRIFs were observed in HR-proficient *KP* tumor cells but not in HR-deficient *KB1P* tumor cells (Figure 7C, upper and lower panel, and 7D; Figure S7E; unpaired
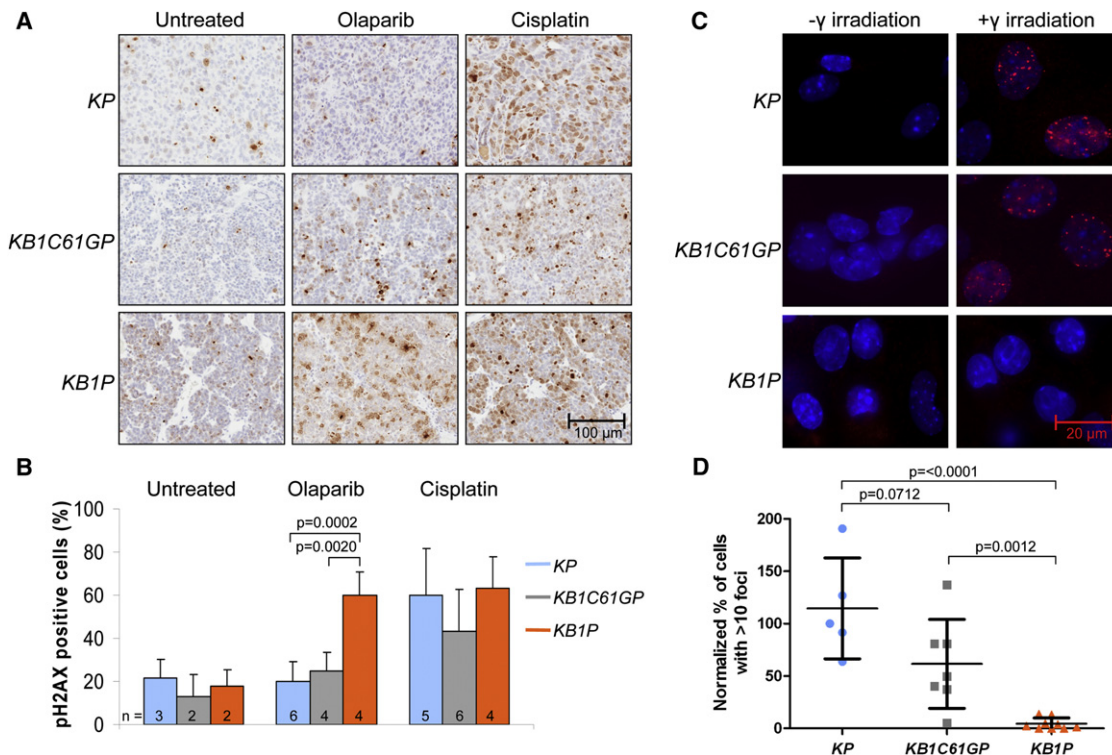
Figure 7. Hypomorphic Activity of BRCA1-C61G In Vivo

(A) Immunohistochemistry of pH2AX foci in *KB1C61GP*, *KB1P*, and *KP* mammary tumors without treatment or after treatment with olaparib or cisplatin. Mice were sacrificed 2 hr after the last of seven daily doses of olaparib (50 mg/kg intraperitoneally) or 24 hr after a single dose of cisplatin (6 mg/kg intravenously).

(B) Quantification of pH2AX foci in *KB1C61GP* (gray), *KB1P* (orange), and *KP* (blue) tumors without treatment or after treatment with olaparib or cisplatin. Error bars indicate SD. n, number of tumors.

(C) Immunofluorescence of RAD51 foci (red) in *KB1C61GP*, *KB1P*, and *KP* tumor cell suspensions with or without γ irradiation (10 Gy). Nuclei were visualized with DAPI (blue).

(D) Quantification of RAD51 foci in *KB1C61GP* (gray; n = 7), *KB1P* (orange; n = 9), and *KP* (blue; n = 5) tumors after γ irradiation. Percentages of cells with >10 RAD51 foci were normalized to tumor cells derived from a *KP* tumor. Error bars indicate SEM. See also Figure S7.

t test p = < 0.0001). Although we have no evidence for residual HR activity of BRCA1-C61G in vitro (Figures S7A–S7D), we did observe RAD51 IRIFs in short-term cultures derived from *KB1C61GP* tumors (Figure 7C, middle panel; Figure S7E). The number of cells with RAD51 foci after irradiation was significantly higher in *KB1C61GP* cells compared to *KB1P* cells (Figure 7D; unpaired t test p = 0.0012). Compared to *KP* tumor cells, *KB1C61GP* cells appeared to have a somewhat lower amount of RAD51-positive cells after irradiation, but this difference did not reach statistical significance (Figure 7D; unpaired t test p = 0.0712).

DISCUSSION

We have studied the importance of BRCA1 RING function in development, tumor suppression, and therapy response using a mouse model carrying the *Brca1^C61G* missense mutation, which impairs BRCA1/BARD1 heterodimerization and ubiquitin ligase activity. Similar to *Brca1* null mutant mice, homozygous *Brca1^C61G* mutants displayed embryonic lethality and heterozygous *Brca1^C61G* mutant mice with tissue-specific loss of *p53* and the second *Brca1* allele developed mammary carcinomas

resembling *Brca1* null tumors. These findings indicate a pronounced loss of function of the mutant BRCA1-C61G protein. However, in contrast to *Brca1* null mammary tumors from *KB1P* mice, *Brca1^C61G* tumors from *KB1C61GP* mice readily became resistant to cisplatin without undergoing genetic reversion of the C61G mutation. The acquired resistance of *Brca1^C61G* tumors to platinum drugs and PARP inhibitors appears to be caused by residual activity of the mutant BRCA1-C61G protein resulting in an altered DNA damage response, as these tumors show reduced levels of pH2AX-positive DNA damage foci after olaparib treatment and formation of DNA damage-induced RAD51 foci.

The Role of BRCA1 RING Activity in Mouse Development and Tumor Suppression

To study the role of BRCA1 in normal development and tumor suppression, a range of conventional *Brca1* knockout mouse models has been generated carrying mutations in different parts of the gene (Drost and Jonkers, 2009; Evers and Jonkers, 2006). Most homozygous *Brca1* mouse mutants show embryonic lethality at mid-gestation, whereas known *Brca1* hypomorphic mutants display a less severe, and in case of the *Brca1^Δexon11*

mutation even partly viable, embryonic phenotype (Hohenstein et al., 2001; Xu et al., 2001). In terms of their developmental phenotype, homozygous *Brca1*^{*C61G*} mutant mice resemble *Brca1* null mutants rather than *Brca1* hypomorphic mutants that still express a partly functional BRCA1 protein. In line with this, Chang et al. (2009) showed that BAC transgenic mice expressing the *Brca1*^{*C61G*} variant failed to rescue the embryonic lethality of *Brca1* knockout mice. Together, these data show that BRCA1 RING activity is essential for embryonic survival.

BRCA1 RING activity is also essential for tumor suppression, because *KB1C61GP* mice developed undifferentiated, ER-negative mammary carcinomas that closely resembled *Brca1* null mammary tumors and human *BRCA1*-mutated breast tumors.

The Role of BRCA1 RING Activity in Therapy Response and Resistance

Although human BRCA1-deficient tumors are very sensitive to DSB-forming agents, they eventually become resistant. Secondary mutations in the *BRCA1* gene appear to be one mechanism for ovarian carcinomas to develop platinum resistance (Swisher et al., 2008), suggesting that restoration of BRCA1 expression is required for resistance to platinum-based chemotherapy. In line with this, *Brca1* null mouse mammary tumors with a large intragenic deletion of *Brca1* exons 5–13 fail to develop resistance and remain hypersensitive to cisplatin or carboplatin even after multiple rounds of treatment (Rottenberg et al., 2007).

We found that *Brca1*^{*C61G*} mammary tumors from *KB1C61GP* mice respond much worse to treatment with olaparib or cisplatin than *Brca1* null tumors from *KB1P* mice. *KB1C61GP* tumors also developed cisplatin resistance, which was never observed in *KB1P* tumors. Surprisingly, we have found no evidence for genetic reversion of *Brca1* by secondary mutations in cisplatin-resistant *KB1C61GP* tumors. The absence of secondary mutations in *Brca1* indicates that *KB1C61GP* tumors may readily acquire resistance to DNA damaging agents due to residual activity of the mutant BRCA1-C61G protein. This residual activity of BRCA1-C61G might relate to another function of BRCA1 besides HR-mediated DNA repair, such as its reported role in gene silencing in constitutive heterochromatin (Zhu et al., 2011). However, we obtained no evidence for restoration of heterochromatin-mediated silencing in therapy-resistant *KB1C61GP* tumors.

It is also possible that more subtle alterations, such as increased expression of BRCA1-C61G or adaptations in the DNA damage response network might suffice to trigger resistance to HRD targeted therapy in *KB1C61GP* tumors. In line with this, we found that cisplatin-resistant *KB1C61GP* tumors were cross-resistant to the clinical PARP inhibitor olaparib, which induces DSBs through inhibition of SSB repair. This finding excludes platinum-specific resistance mechanisms such as increased NER activity (Martin et al., 2008) or reduced expression of the copper transporter CTR1 (Ishida et al., 2010) and advocates for adaptation at the level of HR-mediated DNA repair. Nevertheless, cisplatin-resistant *KB1C61GP* tumors were still sensitive to the bifunctional alkylator nimustine. This might be due to the fact that nimustine causes more ICLs and may therefore be more lethal to cells with decreased HR capacity

than cisplatin (Deans and West, 2011). Consistent with a role in ICL repair, BRCA1 has been shown to associate with FANCD2 (Taniguchi et al., 2002), one of the central proteins in the Fanconi Anemia pathway, and siRNA depletion of BRCA1 results in loss of damage-induced FANCD2 foci (Vandenberg et al., 2003).

Hypomorphic Activity of BRCA1-C61G

We have obtained evidence that residual activity of the mutant BRCA1-C61G protein in the DNA damage response underlies the resistance of *KB1C61GP* tumors to olaparib and cisplatin. Compared to BRCA1-deficient tumors, *KB1C61GP* tumors showed more DNA damage-induced RAD51 foci and fewer pH2AX positive cells, suggesting that the DNA repair process in *KB1C61GP* tumors is (partially) intact. However, basic HR levels of both human (Ransburgh et al., 2010) and mouse C61G mutant cells (Figures S7A and S7B) in vitro are very low. This apparent discrepancy between in vitro HR reporter activity and in vivo response of BRCA1-C61G mutant mammary tumors to DNA damage could be the result of differences between in vivo and in vitro assays or of differences in cell type. Alternatively, additional (epi)genetic alterations might contribute to the altered DNA damage response of BRCA1-C61G mutant tumors.

The mouse model we have used to investigate the in vivo functions of the BRCA1 RING domain carries the *Brca1*^{*C61G*} missense mutation, which mutates the first cysteine residue in the last C-X$_2$-C pair of Zn^{2+} binding ligands within the BRCA1 RING domain (Brzovic et al., 2001). The C61G mutation in the BRCA1 RING domain is one of the most frequently reported missense variants (BIC database; http://research.nhgri.nih.gov/bic/) and linked to the development of breast and ovarian cancer (Castilla et al., 1994; Friedman et al., 1994). This mutation reduces the binding between BRCA1 and BARD1, and inhibits E2 conjugating enzyme interaction and thereby the E3 ubiquitin ligase activity of the heterodimer (Hashizume et al., 2001; Mallery et al., 2002; Ruffner et al., 2001). It is interesting to compare our results to data obtained with the synthetic *Brca1*^{*I26A*} mutation (Reid et al., 2008; Shakya et al., 2011), which is suggested to produce a protein that lacks the E3 ubiquitin ligase activity but retains the ability to heterodimerize with BARD1 (Brzovic et al., 2003; Christensen et al., 2007). Cells expressing BRCA1-I26A are able to repair DSBs by HR at the same level as wild-type cells (Reid et al., 2008), whereas BRCA-C61G mutant cells have a very low HR activity (Figures S7A and S7B) (Ransburgh et al., 2010). Although mammary tumor development is observed in *KB1C61GP* mice expressing BRCA1-C61G, BRCA1-I26A is able to prevent tumor formation to the same degree as wild-type BRCA1 (Shakya et al., 2011). This suggests that not the enzymatic activity but rather another function of the RING domain (e.g., BRCA1/BARD1 heterodimerization) is essential for the tumor suppressive activity of BRCA1.

Clinical Implications

We believe that the work presented in this study may have important diagnostic and therapeutic implications. We show that secondary mutations in the *Brca1* gene are not always required to develop resistance to platinum drugs or PARP inhibitors, as residual activity of BRCA1 mutant proteins with a dysfunctional RING domain may be sufficient for tumor cells to withstand treatment with DNA damaging agents.

Nevertheless, our data indicate that platinum- and olaparib-resistant tumors in $BRCA1^{C61G}$ mutation carriers may still respond to treatment with bifunctional alkylators, like nimustine. This may not only hold true for the $BRCA1^{C61G}$ mutation but also for other pathogenic missense mutations in the BRCA1 RING domain. The fact that $Brca1^{\Delta 11/\Delta 11};p53^{-/-}$ mouse mammary tumors, which only express the BRCA1-Δ11 isoform, can acquire resistance to cisplatin (Shafee et al., 2008) suggests that certain pathogenic missense or splicing mutations outside the BRCA1 RING domain might also produce BRCA1 species with residual activity resulting in an altered DNA damage response. Because it will be difficult to obtain treatment response and survival data for sufficiently large numbers of patients carrying specific $BRCA1$ founder mutations, it will be useful to evaluate the impact of defined $Brca1$ mutations on treatment response and resistance in genetically engineered mouse models for BRCA1-associated breast and ovarian cancer. It will also be interesting to evaluate the response of mouse mammary tumors carrying $Bard1$ mutations to treatment with DSB-forming agents. Shakya et al. (2008) have shown that BARD1-deficient mouse mammary tumors are virtually indistinguishable from BRCA1-deficient tumors. However, it is unknown whether BARD1-deficient tumors have a similar response to DNA damaging agents as BRCA1-deficient tumors.

Currently, it is thought that genomic profiling of tumors may serve as potential diagnostic tool to stratify patients for HRD targeted therapies (Asakawa et al., 2010; Graeser et al., 2010; Lips et al., 2011; Vollebergh et al., 2011). However, here we show that although mouse mammary tumors with different $Brca1$ mutations have identical genomic profiles, they show marked differences in their capacity to form DNA damage-induced RAD51 foci and in their responses to HRD targeted therapy. It may therefore be useful to stratify patients for HRD targeted therapies not only by genomic profiling of tumors but also according to functional assays, like RAD51 foci formation assays, and the precise nature of the underlying $BRCA1$ mutation.

EXPERIMENTAL PROCEDURES

Generation of the $Brca1^{C61G}$ Mutant Mice

Mouse ES cells were targeted with a construct in which $Brca1$ exon 5 was modified by site-directed mutagenesis to encode the C61G mutation (Figure 1). The neomycin selection cassette was removed from correctly targeted cells by Cre-excision. The resulting ES cells were injected into C57BL/6J blastocysts to produce chimeric males, which were mated with C57BL/6J females to generate $Brca1^{C61G/+}$ mice. $Brca1^{C61G/+}$ mice were bred with $K14cre;Brca1^{F/F};$ $p53^{F/F}$ (KB1P) animals (Liu et al., 2007) to generate $K14cre;Brca1^{F/C61G};p53^{F/F}$ (KB1C61GP) mice. Full details on the generation of the $Brca1^{C61G}$ allele are provided in the Supplemental Experimental Procedures.

Orthotopic Transplantations and Drug Interventions

All experiments involving animals comply with local and international regulations and ethical guidelines, and have been authorized by our local animal experimental committee at the Netherlands Cancer Institute (DEC-NKI). Small fragments of mammary tumors from $K14cre;p53^{F/F}$ (KP), KB1P, or KB1C61GP mice were transplanted orthotopically in FVB:129/Ola F1 hybrid female mice as described previously (Rottenberg et al., 2007). When the tumor volume exceeded 200 mm^3, mice were treated with the MTD of cisplatin, olaparib, and nimustine (Evers et al., 2010; Rottenberg et al., 2007, 2008). To study resistance, animals received additional doses of cisplatin when tumors grew back to 200 mm^3. Animals were sacrificed when the tumor volume exceeded 1,500 mm^3 or when they became ill from drug toxicity.

RAD51 Foci Formation Assay

Cells from cryopreserved tumors were grown on glass coverslips for 36–48 hr, γ-irradiated with 10 Gy, and fixed 6 hr later in 2% paraformaldehyde. RAD51 immunofluorescence was performed as described previously (Bouwman et al., 2010). To quantify RAD51 foci in single tumor cells, 150–200 cells per condition were counted blindly. Cells were scored RAD51-positive if they had more than ten RAD51-positive dots per nucleus.

ACCESSION NUMBERS

Array CGH data generated in this study have been deposited at the National Center for Biotechnology Information Gene Expression Omnibus database (http://www.ncbi.nlm.nih.gov/geo) under accession number GSE30710.

SUPPLEMENTAL INFORMATION

Supplemental Information includes three tables, seven figures, and Supplemental Experimental Procedures and can be found with this article online at doi:10.1016/j.ccr.2011.11.014.

REFERENCES

Asakawa, H., Koizumi, H., Koike, A., Takahashi, M., Wu, W., Iwase, H., Fukuda, M., and Ohta, T. (2010). Prediction of breast cancer sensitivity to neoadjuvant chemotherapy based on status of DNA damage repair proteins. Breast Cancer Res. 12, R17.

Bhattacharyya, A., Ear, U.S., Koller, B.H., Weichselbaum, R.R., and Bishop, D.K. (2000). The breast cancer susceptibility gene BRCA1 is required for subnuclear assembly of Rad51 and survival following treatment with the DNA cross-linking agent cisplatin. J. Biol. Chem. 275, 23899–23903.

Bouwman, P., Aly, A., Escandell, J.M., Pieterse, M., Bartkova, J., van der Gulden, H., Hiddingh, S., Thanasoula, M., Kulkarni, A., Yang, Q., et al. (2010). 53BP1 loss rescues BRCA1 deficiency and is associated with triple-negative and BRCA-mutated breast cancers. Nat. Struct. Mol. Biol. 17, 688–695.

Bryant, H.E., Schultz, N., Thomas, H.D., Parker, K.M., Flower, D., Lopez, E., Kyle, S., Meuth, M., Curtin, N.J., and Helleday, T. (2005). Specific killing of BRCA2-deficient tumours with inhibitors of poly(ADP-ribose) polymerase. Nature 434, 913–917.

Brzovic, P.S., Meza, J.E., King, M.C., and Klevit, R.E. (2001). BRCA1 RING domain cancer-predisposing mutations. Structural consequences and effects on protein-protein interactions. J. Biol. Chem. 276, 41399–41406.

Brzovic, P.S., Keeffe, J.R., Nishikawa, H., Miyamoto, K., Fox, D., 3rd, Fukuda, M., Ohta, T., and Klevit, R. (2003). Binding and recognition in the assembly of an active BRCA1/BARD1 ubiquitin-ligase complex. Proc. Natl. Acad. Sci. USA 100, 5646–5651.

Castilla, L.H., Couch, F.J., Erdos, M.R., Hoskins, K.F., Calzone, K., Garber, J.E., Boyd, J., Lubin, M.B., Deshano, M.L., Brody, L.C., et al. (1994). Mutations in the BRCA1 gene in families with early-onset breast and ovarian cancer. Nat. Genet. 8, 387–391.

Chang, S., Biswas, K., Martin, B.K., Stauffer, S., and Sharan, S.K. (2009). Expression of human BRCA1 variants in mouse ES cells allows functional analysis of BRCA1 mutations. J. Clin. Invest. 119, 3160–3171.

Christensen, D.E., Brzovic, P.S., and Klevit, R.E. (2007). E2-BRCA1 RING interactions dictate synthesis of mono- or specific polyubiquitin chain linkages. Nat. Struct. Mol. Biol. 14, 941–948.

de Ronde, J.J., Klijn, C., Velds, A., Holstege, H., Reinders, M.J., Jonkers, J., and Wessels, L.F. (2010). KC-SMARTR: An R package for detection of statistically significant aberrations in multi-experiment aCGH data. BMC Res. Notes 3, 298.

Deans, A.J., and West, S.C. (2011). DNA interstrand crosslink repair and cancer. Nat. Rev. Cancer 11, 467–480.

Drost, R.M., and Jonkers, J. (2009). Preclinical mouse models for BRCA1-associated breast cancer. Br. J. Cancer 101, 1651–1657.

Evers, B., and Jonkers, J. (2006). Mouse models of BRCA1 and BRCA2 deficiency: past lessons, current understanding and future prospects. Oncogene 25, 5885–5897.

Evers, B., Schut, E., van der Burg, E., Braumuller, T.M., Egan, D.A., Holstege, H., Edser, P., Adams, D.J., Wade-Martins, R., Bouwman, P., and Jonkers, J. (2010). A high-throughput pharmaceutical screen identifies compounds with specific toxicity against BRCA2-deficient tumors. Clin. Cancer Res. 16, 99–108.

Fabbro, M., Rodriguez, J.A., Baer, R., and Henderson, B.R. (2002). BARD1 induces BRCA1 intranuclear foci formation by increasing RING-dependent BRCA1 nuclear import and inhibiting BRCA1 nuclear export. J. Biol. Chem. 277, 21315–21324.

Farmer, H., McCabe, N., Lord, C.J., Tutt, A.N., Johnson, D.A., Richardson, T.B., Santarosa, M., Dillon, K.J., Hickson, I., Knights, C., et al. (2005). Targeting the DNA repair defect in BRCA mutant cells as a therapeutic strategy. Nature 434, 917–921.

Fong, P.C., Boss, D.S., Yap, T.A., Tutt, A., Wu, P., Mergui-Roelvink, M., Mortimer, P., Swaisland, H., Lau, A., O'Connor, M.J., et al. (2009). Inhibition of poly(ADP-ribose) polymerase in tumors from BRCA mutation carriers. N. Engl. J. Med. 361, 123–134.

Fong, P.C., Yap, T.A., Boss, D.S., Carden, C.P., Mergui-Roelvink, M., Gourley, C., De Greve, J., Lubinski, J., Shanley, S., Messiou, C., et al. (2010). Poly(ADP)-ribose polymerase inhibition: frequent durable responses in BRCA carrier ovarian cancer correlating with platinum-free interval. J. Clin. Oncol. 28, 2512–2519.

Friedman, L.S., Ostermeyer, E.A., Szabo, C.I., Dowd, P., Lynch, E.D., Rowell, S.E., and King, M.C. (1994). Confirmation of BRCA1 by analysis of germline mutations linked to breast and ovarian cancer in ten families. Nat. Genet. 8, 399–404.

Graeser, M., McCarthy, A., Lord, C.J., Savage, K., Hills, M., Salter, J., Orr, N., Parton, M., Smith, I.E., Reis-Filho, J.S., et al. (2010). A marker of homologous recombination predicts pathologic complete response to neoadjuvant chemotherapy in primary breast cancer. Clin. Cancer Res. 16, 6159–6168.

Hashizume, R., Fukuda, M., Maeda, I., Nishikawa, H., Oyake, D., Yabuki, Y., Ogata, H., and Ohta, T. (2001). The RING heterodimer BRCA1-BARD1 is a ubiquitin ligase inactivated by a breast cancer-derived mutation. J. Biol. Chem. 276, 14537–14540.

Hohenstein, P., Kielman, M.F., Breukel, C., Bennett, L.M., Wiseman, R., Krimpenfort, P., Cornelisse, C., van Ommen, G.J., Devilee, P., and Fodde, R.

(2001). A targeted mouse Brca1 mutation removing the last BRCT repeat results in apoptosis and embryonic lethality at the headfold stage. Oncogene 20, 2544–2550.

Holstege, H., van Beers, E., Velds, A., Liu, X., Joosse, S.A., Klarenbeek, S., Schut, E., Kerkhoven, R., Klijn, C.N., Wessels, L.F., et al. (2010). Cross-species comparison of aCGH data from mouse and human BRCA1- and BRCA2-mutated breast cancers. BMC Cancer 10, 455.

Huen, M.S., Sy, S.M., and Chen, J. (2010). BRCA1 and its toolbox for the maintenance of genome integrity. Nat. Rev. Mol. Cell Biol. 11, 138–148.

Ishida, S., McCormick, F., Smith-McCune, K., and Hanahan, D. (2010). Enhancing tumor-specific uptake of the anticancer drug cisplatin with a copper chelator. Cancer Cell 17, 574–583.

Joukov, V., Chen, J., Fox, E.A., Green, J.B., and Livingston, D.M. (2001). Functional communication between endogenous BRCA1 and its partner, BARD1, during Xenopus laevis development. Proc. Natl. Acad. Sci. USA 98, 12078–12083.

Klijn, C., Holstege, H., de Ridder, J., Liu, X., Reinders, M., Jonkers, J., and Wessels, L. (2008). Identification of cancer genes using a statistical framework for multiexperiment analysis of nondiscretized array CGH data. Nucleic Acids Res. 36, e13.

Lakhani, S.R., Van De Vijver, M.J., Jacquemier, J., Anderson, T.J., Osin, P.P., McGuffog, L., and Easton, D.F. (2002). The pathology of familial breast cancer: predictive value of immunohistochemical markers estrogen receptor, progesterone receptor, HER-2, and p53 in patients with mutations in BRCA1 and BRCA2. J. Clin. Oncol. 20, 2310–2318.

Lips, E.H., Mulder, L., Hannemann, J., Laddach, N., Vrancken Peeters, M.T., van de Vijver, M.J., Wesseling, J., Nederlof, P.M., and Rodenhuis, S. (2011). Indicators of homologous recombination deficiency in breast cancer and association with response to neoadjuvant chemotherapy. Ann. Oncol. 22, 870–876.

Liu, X., Holstege, H., van der Gulden, H., Treur-Mulder, M., Zevenhoven, J., Velds, A., Kerkhoven, R.M., van Vliet, M.H., Wessels, L.F., Peterse, J.L., et al. (2007). Somatic loss of BRCA1 and p53 in mice induces mammary tumors with features of human BRCA1-mutated basal-like breast cancer. Proc. Natl. Acad. Sci. USA 104, 12111–12116.

Mallery, D.L., Vandenberg, C.J., and Hiom, K. (2002). Activation of the E3 ligase function of the BRCA1/BARD1 complex by polyubiquitin chains. EMBO J. 21, 6755–6762.

Martin, L.P., Hamilton, T.C., and Schilder, R.J. (2008). Platinum resistance: the role of DNA repair pathways. Clin. Cancer Res. 14, 1291–1295.

Morris, J.R., and Solomon, E. (2004). BRCA1 : BARD1 induces the formation of conjugated ubiquitin structures, dependent on K6 of ubiquitin, in cells during DNA replication and repair. Hum. Mol. Genet. 13, 807–817.

Moynahan, M.E., Chiu, J.W., Koller, B.H., and Jasin, M. (1999). Brca1 controls homology-directed DNA repair. Mol. Cell 4, 511–518.

Moynahan, M.E., Cui, T.Y., and Jasin, M. (2001). Homology-directed DNA repair, mitomycin-c resistance, and chromosome stability is restored with correction of a Brca1 mutation. Cancer Res. 61, 4842–4850.

Nelson, A.C., and Holt, J.T. (2010). Impact of RING and BRCT domain mutations on BRCA1 protein stability, localization and recruitment to DNA damage. Radiat. Res. 174, 1–13.

Rahman, N., and Stratton, M.R. (1998). The genetics of breast cancer susceptibility. Annu. Rev. Genet. 32, 95–121.

Ransburgh, D.J., Chiba, N., Ishioka, C., Toland, A.E., and Parvin, J.D. (2010). Identification of breast tumor mutations in BRCA1 that abolish its function in homologous DNA recombination. Cancer Res. 70, 988–995.

Reid, L.J., Shakya, R., Modi, A.P., Lokshin, M., Cheng, J.T., Jasin, M., Baer, R., and Ludwig, T. (2008). E3 ligase activity of BRCA1 is not essential for mammalian cell viability or homology-directed repair of double-strand DNA breaks. Proc. Natl. Acad. Sci. USA 105, 20876–20881.

Rottenberg, S., Nygren, A.O., Pajic, M., van Leeuwen, F.W., van der Heijden, I., van de Wetering, K., Liu, X., de Visser, K.E., Gilhuijs, K.G., van Tellingen, O., et al. (2007). Selective induction of chemotherapy resistance of mammary

tumors in a conditional mouse model for hereditary breast cancer. Proc. Natl. Acad. Sci. USA *104*, 12117–12122.

Rottenberg, S., Jaspers, J.E., Kersbergen, A., van der Burg, E., Nygren, A.O., Zander, S.A., Derksen, P.W., de Bruin, M., Zevenhoven, J., Lau, A., et al. (2008). High sensitivity of BRCA1-deficient mammary tumors to the PARP inhibitor AZD2281 alone and in combination with platinum drugs. Proc. Natl. Acad. Sci. USA *105*, 17079–17084.

Rottenberg, S., Pajic, M., and Jonkers, J. (2010). Studying drug resistance using genetically engineered mouse models for breast cancer. Methods Mol. Biol. *596*, 33–45.

Ruffner, H., Joazeiro, C.A., Hemmati, D., Hunter, T., and Verma, I.M. (2001). Cancer-predisposing mutations within the RING domain of BRCA1: loss of ubiquitin protein ligase activity and protection from radiation hypersensitivity. Proc. Natl. Acad. Sci. USA *98*, 5134–5139.

Sakai, W., Swisher, E.M., Karlan, B.Y., Agarwal, M.K., Higgins, J., Friedman, C., Villegas, E., Jacquemont, C., Farrugia, D.J., Couch, F.J., et al. (2008). Secondary mutations as a mechanism of cisplatin resistance in BRCA2-mutated cancers. Nature *451*, 1116–1120.

Sakai, W., Swisher, E.M., Jacquemont, C., Chandramohan, K.V., Couch, F.J., Langdon, S.P., Wurz, K., Higgins, J., Villegas, E., and Taniguchi, T. (2009). Functional restoration of BRCA2 protein by secondary BRCA2 mutations in BRCA2-mutated ovarian carcinoma. Cancer Res. *69*, 6381–6386.

Shafee, N., Smith, C.R., Wei, S., Kim, Y., Mills, G.B., Hortobagyi, G.N., Stanbridge, E.J., and Lee, E.Y. (2008). Cancer stem cells contribute to cisplatin resistance in Brca1/p53-mediated mouse mammary tumors. Cancer Res. *68*, 3243–3250.

Shakya, R., Reid, L.J., Reczek, C.R., Cole, F., Egli, D., Lin, C.S., deRooij, D.G., Hirsch, S., Ravi, K., Hicks, J.B., et al. (2011). BRCA1 tumor suppression depends on BRCT phosphoprotein binding, but not its E3 ligase activity. Science *334*, 525–528.

Shakya, R., Szabolcs, M., McCarthy, E., Ospina, E., Basso, K., Nandula, S., Murty, V., Baer, R., and Ludwig, T. (2008). The basal-like mammary carcinomas induced by Brca1 or Bard1 inactivation implicate the BRCA1/BARD1 heterodimer in tumor suppression. Proc. Natl. Acad. Sci. USA *105*, 7040–7045.

Swisher, E.M., Sakai, W., Karlan, B.Y., Wurz, K., Urban, N., and Taniguchi, T. (2008). Secondary BRCA1 mutations in BRCA1-mutated ovarian carcinomas with platinum resistance. Cancer Res. *68*, 2581–2586.

Taniguchi, T., Garcia-Higuera, I., Andreassen, P.R., Gregory, R.C., Grompe, M., and D'Andrea, A.D. (2002). S-phase-specific interaction of the Fanconi anemia protein, FANCD2, with BRCA1 and RAD51. Blood *100*, 2414–2420.

Tirkkonen, M., Johannsson, O., Agnarsson, B.A., Olsson, H., Ingvarsson, S., Karhu, R., Tanner, M., Isola, J., Barkardottir, R.B., Borg, A., and Kallioniemi, O.P. (1997). Distinct somatic genetic changes associated with tumor progression in carriers of BRCA1 and BRCA2 germ-line mutations. Cancer Res. *57*, 1222–1227.

Tutt, A., Robson, M., Garber, J.E., Domchek, S.M., Audeh, M.W., Weitzel, J.N., Friedlander, M., Arun, B., Loman, N., Schmutzler, R.K., et al. (2010). Oral poly(ADP-ribose) polymerase inhibitor olaparib in patients with BRCA1 or BRCA2 mutations and advanced breast cancer: a proof-of-concept trial. Lancet *376*, 235–244.

Vandenberg, C.J., Gergely, F., Ong, C.Y., Pace, P., Mallery, D.L., Hiom, K., and Patel, K.J. (2003). BRCA1-independent ubiquitination of FANCD2. Mol. Cell *12*, 247–254.

Vollebergh, M.A., Lips, E.H., Nederlof, P.M., Wessels, L.F., Schmidt, M.K., van Beers, E.H., Cornelissen, S., Holtkamp, M., Froklage, F.E., de Vries, E.G., et al. (2011). An aCGH classifier derived from BRCA1-mutated breast cancer and benefit of high-dose platinum-based chemotherapy in HER2-negative breast cancer patients. Ann. Oncol. *22*, 1561–1570.

Xia, Y., Pao, G.M., Chen, H.W., Verma, I.M., and Hunter, T. (2003). Enhancement of BRCA1 E3 ubiquitin ligase activity through direct interaction with the BARD1 protein. J. Biol. Chem. *278*, 5255–5263.

Xu, X., Qiao, W., Linke, S.P., Cao, L., Li, W.M., Furth, P.A., Harris, C.C., and Deng, C.X. (2001). Genetic interactions between tumor suppressors Brca1 and p53 in apoptosis, cell cycle and tumorigenesis. Nat. Genet. *28*, 266–271.

Zhu, Q., Pao, G.M., Huynh, A.M., Suh, H., Tonnu, N., Nederlof, P.M., Gage, F.H., and Verma, I.M. (2011). BRCA1 tumour suppression occurs via heterochromatin-mediated silencing. Nature *477*, 179–184.